Title: An Approach to Tree Detection Based on the Fusion of Multitemporal LiDAR Data

This letter appears in: IEEE Geoscience and Remote Sensing Letters

Date of Publication: 25 April 2019

Author(s): Daniele Marinelli, Claudia Paris, Lorenzo Bruzzone

Volume:

Page(s):

DOI: 10.1109/LGRS.2019.2908314

An Approach to Tree Detection Based on the Fusion of Multitemporal LiDAR Data

Daniele Marinelli, *Student Member, IEEE,* Claudia Paris, *Member, IEEE,*
Lorenzo Bruzzone, *Fellow, IEEE*

***Abstract*—The repetitive acquisition of airborne Light Detection and Ranging (LiDAR) data for forest surveys is rapidly increasing, thus making possible the forest dynamic analysis. Moreover, the availability of multitemporal data enables the possibility to improve the forest attribute estimates performed at single date, especially when one LiDAR acquisition has a lower pulse density with respect to the other. This letter presents a novel approach that exploits the bi-temporal data information to: (i) improve the tree detection at both dates, and (ii) identify forest changes at single tree level. This is done by using a novel compound approach to the detection of trees in bi-temporal data based on the Bayes rule for minimum error. Significant geometric features are extracted for each candidate tree-top and are used to estimate statistical terms employed in the compound approach. The multitemporal information is considered by estimating (in an iterative way) the probabilities of transition, which take into account the temporal dependence between the LiDAR acquisitions. The proposed approach is evaluated on multitemporal LiDAR data acquired in a coniferous forest located in the Southern Italian Alps. Experimental results confirm the effectiveness of the compound detection that increases the overall accuracy (OA) up to 8.6% with respect to the single-date detection.**

***Index Terms*—Multitemporal analysis, tree-top detection, compound classification, change detection, Light Detection and Ranging (LiDAR), remote sensing, forestry.**

I. Introduction

Airborne Light Detection and Ranging (LiDAR) has been extensively used to perform surveys on large forests, because of its capability of directly measure the 3-D distribution of the trees [1]. Due to the reduction of the acquisition costs of these data and the standardization of their processing, repeated acquisitions are now taken more and more frequently over large areas [2]. The availability of multitemporal LiDAR data allows for the assessment of forest dynamics, which is crucial for forest monitoring. Many techniques have been developed for forest monitoring with LiDAR data [3]–[7]. In [3] the authors demonstrate the utility and huge potential of repeated LiDAR data acquisitions for forest resource monitoring and carbon management. Four airborne LiDAR surveys acquired from 2002 to 2012 over a region in Scotland were used to successfully monitor tree growth, biomass dynamics and carbon change both at stand and tree levels. Plot level analysis allows for quantification of average tree height/volume growth or biomass dynamic at stand level (e.g., 30×30 m) [4]. In contrast, several studies successfully used tree level analysis to monitor the growth of tree height, canopy height and crown area [5]–[7].

However, performing tree level analysis on multitemporal LiDAR acquisitions is a complex task [8]. While in recent years medium (e.g., 10 pulses/m^2) and high pulse density ($\geq$ 20 pulses/m^2) data are typically acquired, older data may be characterized by low pulse densities ($\leq$ 5 pulses/m^2), which prevent such refined multitemporal analysis. At plot scale, different pulse densities do not heavily impact on the estimation of forest attributes [4]. In contrast, at tree level low pulse density acquisitions strongly affect forest dynamic parameters estimation. Unrealistic or wrong estimates of tree growth may be obtained due to the probability of missing tree-tops as pulse density decreases [3], [9]. This limits the use of old datasets for performing long-term forest analysis. In this context, it is extremely important to define methods that can fully take advantage of the multitemporal acquisitions to improve the attribute estimation performed at single date before proceeding with the forest trend analysis. In [8], Marinelli *et al.* demonstrated the importance of fusing the information of the two dates before performing the change analysis.

In this letter, we propose an automatic fusion approach that exploits bi-temporal LiDAR data to accurately detect the tree-tops at both dates. The proposed method takes advantage of the multitemporal information to: (i) improve the accuracy of the tree detection performed at single date and (ii) detect the presence of forest changes at tree level. This is done by first separately detecting the trees at both dates. Then, for each tree detected at least at one date, we perform a morphological analysis to extract geometric features from both scenes. Finally, a Bayesian compound decision rule approach is used to estimate the probability that candidate trees are correctly identified in each LiDAR acquisition. Note that the proposed approach accurately detects the trees only trough their tree-tops, paving way to an accurate tree crown segmentation. The method has been tested on a real multitemporal LiDAR dataset acquired with different pulse densities, i.e., in 2007 (5 pulses/m^2) and 2008 (0.48 pulses/m^2). Simulated changes of forest cut and regrowth were introduced to test the capability of the method to accurately detect changes.

II. Problem Formulation

In this section we formalize the tree detection compound problem and define the notation used in the letter. After pre-processing, which includes point cloud registration, normalization and rasterization, we obtain two rasters Canopy Height Models (CHMs) X^1 and X^2 derived from the LiDAR point

clouds acquired at times t_1 and t_2, respectively. After the tree-top detection applied separately to X^1 and X^2, we obtain two sets of candidate tree-tops described by their 2-D (x, y) coordinates that are compared and fused to obtain two sets $\mathcal{S}^1$ and $\mathcal{S}^2$. The fusion is done differently considering two possible cases: i) the same candidate tree-top is identified at both dates; ii) a candidate tree-top is identified at only one date. The first case is identified when for a candidate tree-top detected at t_1 there is a correspondent candidate tree-top at time t_2 at a 2-D Euclidean distance smaller than a given threshold T_s [8]. In this case, each of the two candidate tree-tops is added to the corresponding set. The second case occurs when a candidate tree-top has not a corresponding one at the other date; this case should be better studied by analyzing the crown morphology at both dates. To this end, each candidate tree-top for which no match is found at the other date is added to both the sets $\mathcal{S}^1$ and $\mathcal{S}^2$ (i.e., the same position is considered at both dates). The results of the fusion are two sets of candidate tree-tops $\mathcal{S}^1 = \{\mathbf{s}_k^1\}_{k=1}^K$ and $\mathcal{S}^2 = \{\mathbf{s}_k^2\}_{k=1}^K$ where $\mathbf{s}_k^t = (x_k^t, y_k^t)$ $(t \in \{1, 2\})$ represents the location of the kth candidate tree-top at time t.

Let $\Omega = \{\omega_0^t, \omega_1^t\}$, $(t \in \{1, 2\})$ be the set of possible classes at time t_1 and t_2, where ω_0^t and ω_1^t represent the presence and the absence of a tree-top at time t, respectively. The aim of the proposed approach is to exploit the multitemporal information to perform a compound decision assigning to each candidate tree-top in the sets $\mathcal{S}^1$ and $\mathcal{S}^2$ a class in Ω. For each pair $(\mathbf{s}_k^1, \mathbf{s}_k^2)$, it is possible to identify four cases determined by the pair of labels assigned to it: i) (ω_0^1, ω_0^2) that identifies the presence of a tree at both dates; ii) (ω_0^1, ω_1^2) that identifies the presence of a tree at time t_1 and its absence at time t_2 (i.e., forest cut); iii) (ω_1^1, ω_0^2) that represents the absence of a tree at time t_1 and its presence at time t_2 (i.e., forest regrowth); iv) (ω_1^1, ω_1^2) that represent the absence of trees at both dates.

III. Proposed Tree Detection Compound Approach

A. Bayesian Framework to Compound Tree Detection

Let $\mathbf{f}_k^t$, $(t \in \{1, 2\})$ be the set of geometric features extracted for the kth tree-top at time t used to determine if a tree-top belongs to ω_0 or ω_1 at time t. Let us focus the attention on the kth pair of candidate tree-tops pixel $(\mathbf{s}_k^1, \mathbf{s}_k^2)$ described by the set of features $(\mathbf{f}_k^1, \mathbf{f}_k^2)$. The Bayesian decision rule for compound classification identifies the optimal pair of labels (ω_b^1, ω_e^2) (with $b, e \in \{0, 1\}$) by maximizing the joint posterior probability that models the temporal correlation:

$$(\mathbf{s}_k^1, \mathbf{s}_k^2) \in (\omega_b^1, \omega_e^2) \text{ if } (\omega_b^1, \omega_e^2) = \underset{\omega_i^1, \omega_j^2 \in \Omega}{\operatorname{argmax}} \{P(\omega_i^1, \omega_j^2 | \mathbf{f}_k^1, \mathbf{f}_k^2)\} \quad (1)$$

where $P(\omega_i^1, \omega_j^2 | \mathbf{f}_k^1, \mathbf{f}_k^2)$ is the joint conditional posterior probability of the pair of classes (ω_i^1, ω_j^2) given the feature vectors of the kth tree-top $(\mathbf{f}_k^1, \mathbf{f}_k^2)$. The pair of classes (ω_b^1, ω_e^2) that maximizes (1) is the same that maximizes:

$$(\omega_b^1, \omega_e^2) = \underset{\omega_i^1, \omega_j^2 \in \Omega}{\operatorname{argmax}} \left\{ \frac{p(\mathbf{f}_k^1, \mathbf{f}_k^2 | \omega_i^1, \omega_j^2) P(\omega_j^2 | \omega_i^1) P(\omega_i^1)}{p(\mathbf{f}_k^1, \mathbf{f}_k^2)} \right\} \quad (2)$$

where the joint density $p(\mathbf{f}_k^1, \mathbf{f}_k^2)$ can be neglected since it is not dependent on (ω_i^1, ω_j^2). In the considered tree-top detection problem, it is reasonable to assume temporal class-conditional independence since the feature vector $\mathbf{f}_k^t$ depends only on the characteristics of the CHM at time t. This allows us to rewrite:

$$p(\mathbf{f}_k^1, \mathbf{f}_k^2 | \omega_i^1, \omega_j^2) = p(\mathbf{f}_k^1 | \omega_i^1) p(\mathbf{f}_k^2 | \omega_j^2) \quad (3)$$

where $p(\mathbf{f}_k^1 | \omega_i^1)$ and $p(\mathbf{f}_k^2 | \omega_j^2)$ are the single-date class-conditional density functions. By substituting (3) into (2) and applying some simple statistic, we obtain the following decision rule:

$$(\omega_b^1, \omega_e^2) = \underset{\omega_i^1, \omega_j^2 \in \Omega}{\operatorname{argmax}} \left\{ \frac{P(\omega_i^1 | \mathbf{f}_k^1) P(\omega_j^2 | \mathbf{f}_k^2) P(\omega_j^2 | \omega_i^1)}{P(\omega_j^2)} \right\} \quad (4)$$

Note that the considered compound approach has been widely employed to classify multitemporal images. To apply the Bayesian decision rule for compound classification, we need to estimate all the terms involved in (4) in an unsupervised way. In the considered implementation, we estimate $P(\omega_j^2)$, $P(\omega_i^1 | \mathbf{f}_k^1)$ and $P(\omega_j^2 | \mathbf{f}_k^2)$ on the basis of a model translated in a set of rules which are applied to the feature vectors $(\mathbf{f}_k^1, \mathbf{f}_k^2)$. $P(\omega_j^2 | \omega_i^1)$ is estimated using an iterative algorithm which does not require any *a priori* knowledge about probabilities of transitions. The estimation approach is described in the next subsection.

B. Rule-Based Approach to the Probability Estimation

Although LiDAR data allow for relatively accurate tree-top identification results, detection errors are unavoidable due to upper branches that may lead to false local maxima (i.e., commission errors) or missed smooth tree-tops (i.e., omission errors). Accordingly, we perform a geometric analysis that allows us to evaluate how prominent the candidate tree-top is with respect to the surrounding local maxima. We use this analysis to compute an estimate of the likelihood of a candidate to be a real tree-top.

Let us focus on the kth candidate tree-top $\mathbf{s}_k^t$ which has pixel location (x_k^1, y_k^1) and (x_k^2, y_k^2) in X^1 and X^2, respectively. To model the geometric characteristics of $\mathbf{s}_k^1$ and $\mathbf{s}_k^2$ in the CHMs, we analyze the tree crown profiles along the four main directions (0°, 45°, 90°, 135°) centered in the candidate tree-top position (see Fig. 1). For each crown profile (made up of the CHM pixels values belonging to the considered direction) we detect the local maximum (i.e., highest height value of the profile). Let $\mathbf{f}_k^t = \{d_{k,l}^t\}_{l=1}^4$ be the feature vector made up of the four 2-D Euclidean distances computed in the (x, y) plane between the candidate tree-top position (x_k^t, y_k^t) and the positions of the local maxima, extracted separately at time t_1 and t_2 for the kth tree-top $\mathbf{s}_k^t$. To estimate the prior and the posterior probabilities of the classes $\{\omega_i^1, \omega_j^2\}$ at time t_1 and t_2 we use a set of rules applied to $\mathbf{f}_k^1$ and $\mathbf{f}_k^2$, respectively. In particular, we compute the likelihood that $\mathbf{s}_k^t$ is a tree-top as follows:

$$\ell_k^t = \begin{cases} 0.1 & R = 0 \\ R \cdot 0.25 & 1 \leq R \leq 4 \end{cases}, \text{ with } R = \left| l : d_{k,l}^t \leq T_d \right| \quad (5)$$

where $|\cdot|$ is the cardinality of the set (the number of indexes l for which $d^t_{k,l}$ satisfies the condition) and T_d is a threshold on the distance between the local maximum and the candidate tree-top that allows us to model the prominence of the candidate tree-top. Fig. 1 shows a qualitative example of feature extraction where for each profile, $d^t_{k,l}$ is computed as the distance of the orange dot (local maximum) from the candidate tree-top. In Fig. 1a (true tree-top) 3 profiles present their local maxima in the tree-top location ($\ell^t_k = 0.75$), whereas in Fig. 1b (false tree-top) only one profile corresponds to candidate the tree-top location ($\ell^t_k = 0.25$).

We use the likelihood measure as an approximation of the posterior probabilities, i.e., $P(\omega^t_0|\mathbf{f}^t_k) = \ell^t_k$ and $P(\omega^t_1|\mathbf{f}^t_k) = 1 - \ell^t_k$. According to the considered set of rules, the prior probabilities can be estimated as $P(\omega^2_0) = \left|k : \ell^2_k \geq T_\ell\right| / K$ and $P(\omega^2_1) = \left|k : \ell^2_k < T_\ell\right| / K$ where T_ℓ is a threshold on the likelihood.

C. Iterative Compound Tree Detection Algorithm

In this step, we estimate the elements of the 2×2 matrix of probabilities of transitions at each iteration n:

$$M^n = \begin{bmatrix} P(\omega^2_0 \mid \omega^1_0) & P(\omega^2_1 \mid \omega^1_0) \\ P(\omega^2_0 \mid \omega^1_1) & P(\omega^2_1 \mid \omega^1_1) \end{bmatrix} \quad (6)$$

where the matrix element m^n_{ij} represents the probability that a pixel belongs to the class ω^1_i at time t_1 and to the class ω^2_j at time t_2 at the nth iteration. Note that $P(\omega^2_0|\omega^1_0)$ models the probability that a tree detected in X^1 is still a tree in X^2, $P(\omega^2_0|\omega^1_1)$ models the appearance of new trees, $P(\omega^2_1|\omega^1_0)$ represents the probability that a tree is no more present in X^2 (e.g., forest cut) and $P(\omega^2_1|\omega^1_1)$ represents the probability that the candidate tree-top is actually not a tree-top at both dates. To estimate the probabilities of transition from the multitemporal LiDAR dataset under analysis, we considered the following iterative procedure:

1) Initialization: the posterior probabilities $P(\omega^1_i|\mathbf{f}^1_k)$ and $P(\omega^2_j|\mathbf{f}^2_k)$ and the prior probability $P(\omega^2_j)$ are estimated according to the morphological approach described in III-B. For the initialization we assume the independence of the classes ω^2_j, $(j \in \{0,1\})$ at time t_2 and ω^1_i $(i \in \{0,1\})$ at time t_1. Accordingly, the probabilities of transition is initialized as follows:

$$M^0 = \begin{bmatrix} P(\omega^2_0) & P(\omega^2_1) \\ P(\omega^2_0) & P(\omega^2_1) \end{bmatrix} \quad (7)$$

where the apex 0 indicates the initial iteration. By considering the above initialization, the compound classification results in the assignment of the label $\in \{\omega^t_0, \omega^t_1\}$, $(t \in \{1,2\})$ that maximizes Equation (4) for each $\mathbf{s}^t_k$, $(t \in \{1,2\})$.

2) nth Iteration: the result obtained at iteration $n-1$, can be used to compute the estimate of the probabilities of transition at iteration n, according to the following equation:

$$m^n_{ij} = \frac{\left|k : \mathbf{s}^1_k \text{ assigned to } \omega^1_i \wedge \mathbf{s}^2_k \text{ assigned to } \omega^2_j\right|}{\left|k : \mathbf{s}^1_k \text{ assigned to } \omega^1_i\right|} \quad (8)$$

where $\wedge$ is the *and* operator. Note that the estimates of $P(\omega^1_i|\mathbf{f}^1_k)$,$P(\omega^2_j|\mathbf{f}^2_k)$ and $P(\omega^2_j)$ do not change with the iterations. This is because their values are based on the feature vectors (as shown in III-B) that do not vary with the iterations.

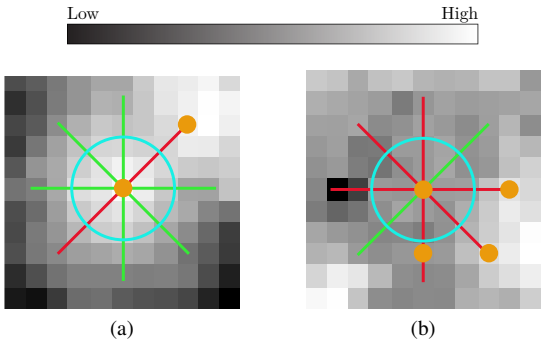

Fig. 1. Example of features extraction for: (a) true tree-top; (b) false tree-top. The lines represent the 4 profiles and the orange dots represent position of the maximum along each profile. The blue circle has a radius equal to T_d. The lines are red if $d^t_{k,l} > T_d$ and green if $d^t_{k,l} \leq T_d$. In (a) 3 out of the 4 maximum positions correspond to the tree-top location, whereas in (b) only 1 out of the 4 maximum positions correspond to the tree-top location.

3) Stop Criterion: the iterative compound tree detection algorithm stops when the largest difference among the estimates of all probabilities of transitions between two consecutive iterations is lower than a certain threshold ϵ:

$$\max_{i \in \{0,1\}, j \in \{0,1\}} \{m^n_{ij} - m^{n-1}_{ij}\} < \epsilon \quad (9)$$

At the end of the procedure, the compound detection result identifies the tree-top obtained for both t_1 and t_2. It is worth noting that the considered formulation allows us to detect: (i) the presence of the tree-tops in the multitemporal CHMs separately, and (ii) the forest changes at tree level.

IV. Experiments and Results

A. Dataset Description

To evaluate the effectiveness of the proposed tree-top detection compound method, we considered a bi-temporal LiDAR dataset acquired in a coniferous forest located at Parco Naturale Paneveggio - Pale di San Martino, Trento, Southern Italian Alps. The coordinates of the central point of the area are $46°17'47{,}60''$ N, $11°45'29{,}98''$ E. The area extends for 368 Ha and the altitude ranges between 1536 m and 2065 m. The dominant species are Norway Spruce and Silver Fir. The first LiDAR survey was done specifically for forest analysis on September 4^{th}, 2007 with the Optech ALTM3100EA instrument by guaranteeing a mean pulse density of 5 pulses/m^2. For each laser pulse four returns were recorded. A digital terrain model (DTM) of the investigated area, with a spatial resolution of 1 m, was extracted from the LiDAR data. The second LiDAR survey was conducted over the whole Province of Trento between October 2007 and December 2008 with an Optech ALTM 3100C. The pulse density was about 0.48 pulses/m^2. For each emitted pulse, both first and last returns were recorded.

The experimental analysis was conducted on 16 circular forest plots (20 m radius) randomly spread over the area, where ground data are available. The position with respect to the center of the sample plot, the tree-top height and the species were recorded for each surveyed tree. The point cloud registration was performed using the Iterative Closest Point

(ICP) algorithm. For details please refer to [8]. The tree-top detection was performed using a Level Set Method [10]. Both the LiDAR acquisitions were rasterized at 0.5 m resolution.For the directional analysis of the crown area around the tree-tops, the length of each profile (from end to end) was 2.5 m. The threshold values T_s, T_d and T_ℓ were set equal to 1.5, 0.75 and 0.3, respectively, while ϵ was set equal to 0.001. Cut of trees and forest regrowth phenomena were simulated to test the robustness of the proposed approach in detecting forest changes. The simulation was done by manually replacing trees (at times t_1 and t_2) from the CHM with terrain. We simulated (between t_1 and t_2) around 10% of cut trees and 10% of planted trees. Note that few non-simulated changes were already present. The numerical results are presented in terms of Omission Errors (OE), Commission Errors (CE) and Overall Accuracy (OA).

B. Results

The results obtained with the proposed method were compared with: (i) the tree-top detection performed independently at each single date and (ii) the merging of the tree-tops separately detected at both dates. Tables Ia and Ib show the numerical results in terms of CE, OE and OA obtained at times t_1 and t_2, respectively. As expected, the OE value at time t_1 is quite similar for the single date case and the proposed compound approach due to relatively high pulse density of the t_1 LiDAR acquisition. However, even though most of the OE trees cannot be easily identified in the CHM (e.g., they are partially covered by other higher trees), the proposed method reduces the OE without increasing the CE errors. In contrast, the merging technique shows a significant increase of CE errors due to the fact that the merging is not able to detect changes and thus all the trees not present at t_1 but present at t_2 are counted as tree-tops also at t_1. The OA shows that the proposed method has better results compared to the single date case.

Considering time t_2 (Table Ib), the OA produced by the proposed method is sharply higher than that of the single date case, thus proving the importance of the multitemporal information. Indeed, due to the low density of the t_2 acquisition, there is a high number of tree-tops missed by the LiDAR sensor which leads to a high number of OE when only the information of the single date is used. By using the multitemporal information the proposed approach uses the information of the high density data to reduce the OE but also the CE. The merging is capable of recovering more missed trees with respect to the proposed method. However, this comes at the cost of a strong increase of the number of CE, which at the end leads to a decrease of the OA.

Fig. 2 shows the map of detected trees results for 4 plots, where the set of fused tree-tops are overlapped on the CHMs of time t_1 and t_2 and represented with different colors, according to the type of multitemporal transition. The qualitative analysis confirms the results obtained from the quantitative view point. The method accurately identifies all the changes (i.e., tree cuts (ω_0^1, ω_1^2) and planting of trees (ω_1^1, ω_0^2)). Moreover, almost all the trees that are present at both dates are correctly identified as unchanged.

Table II shows the error matrix related to the transitions obtained by the proposed compound method. The proposed approach identifies almost all the changed trees. The tree-tops wrongly identified as changed (i.e., the 22 pixels identified as (ω_0^1, ω_1^2)) are trees clearly visible at one date but not well represented by the CHM at the other date. Therefore the compound approach identifies this variation of the posterior probability as a change. Note that the candidate tree-tops that are CE at both dates are identified as trees at both dates or as changed trees (i.e., 11 pixels identified as (ω_0^1, ω_0^2), 2 pixels identified as (ω_0^1, ω_1^2) and 14 pixels identified as (ω_1^1, ω_0^2)) . This is due to two main reasons: (i) at least at one date they have a high $P(\omega_0^t|\mathbf{f}_k^t)$ (due to a local maximum present in the CHM caused typically by rasterization errors); (ii) the Level Set Method detects few CE and therefore $P(\omega_1^2|\omega_1^1)$ has typically very low values (or is equal to 0).

TABLE I
OMISSION ERRORS (OE), COMMISSION ERRORS (CE) AND OVERALL ACCURACY (OA) OBTAINED IN TERMS OF NUMBER (#) AND PERCENTAGE (%): (a) AT TIME t_1; (b) AT TIME t_2. THE PROPOSED COMPOUND METHOD (COMPOUND) IS COMPARED WITH THE TREE-TOP DETECTION OBTAINED ON THE SINGLE ACQUISITION (SINGLE DATE) AND THE SIMPLE INTEGRATION OF THE TREE-TOPS DETECTED IN BOTH DATES (MERGE).

(a)

Approach	Trees	OE		CE		OA
	#	#	%	#	%	%
Single Date	487	79	16.2	5	1	82.9
Merge	487	66	13.6	74	15.2	75
Compound	487	68	14	5	1	**85.2**

(b)

Approach	Trees	OE		CE		OA
	#	#	%	#	%	%
Single Date	484	111	22.9	30	6.2	72.6
Merge	484	65	13.4	79	16.3	74.4
Compound	484	79	16.3	15	3.1	**81.2**

V. CONCLUSION

In this letter, we have proposed a novel automatic approach to the accurate tree detection on multitemporal LiDAR data which is based on a compound approach. The compound

TABLE II
ERROR MATRIX RELATED TO CLASS TRANSITIONS OBTAINED BY THE PROPOSED COMPOUND APPROACH.

		Reference			
		(ω_0^1, ω_0^2)	(ω_0^1, ω_1^2)	(ω_1^1, ω_0^2)	(ω_1^1, ω_1^2)
Compound	(ω_0^1, ω_0^2)	334	1	0	11
	(ω_0^1, ω_1^2)	22	55	0	2
	(ω_1^1, ω_0^2)	0	0	60	14
	(ω_1^1, ω_1^2)	0	0	0	0

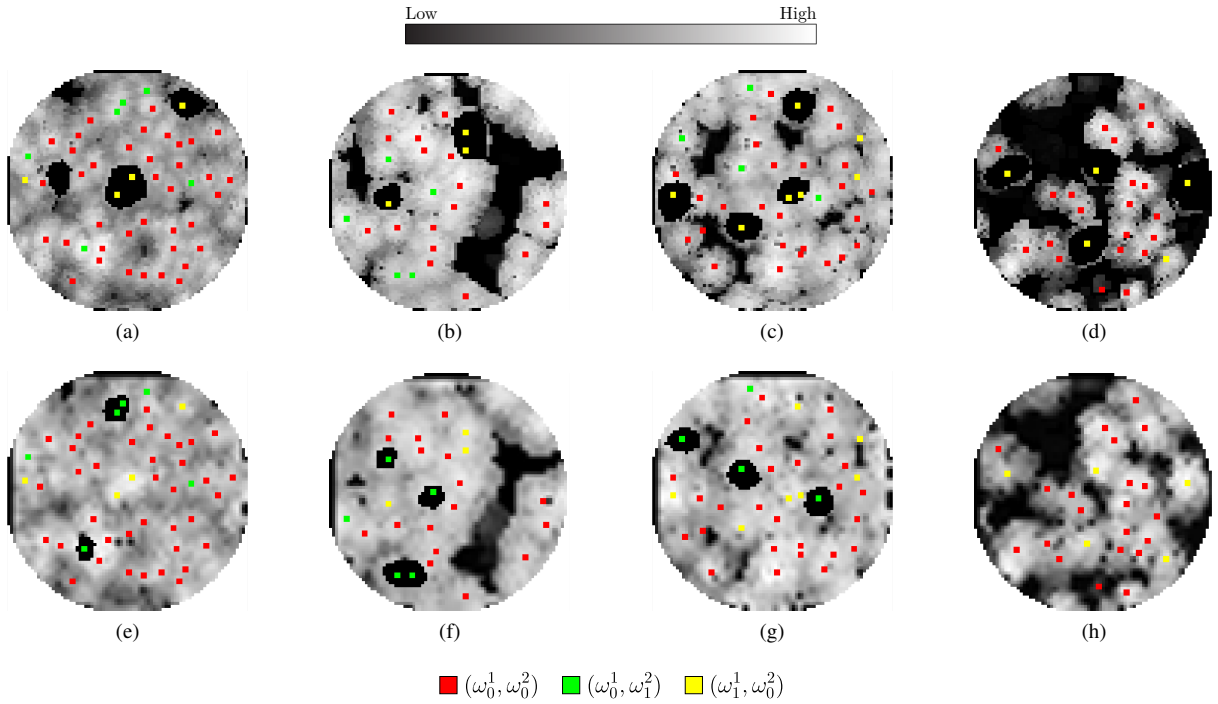

Fig. 2. Example of compound tree detection maps in 4 plots: (a-d) t_1 CHMs; (e-h) t_2 CHMs. The colored dots represent the tree-top positions with the color representing the type of transition.

approach allows us to model temporal dependence of a tree-top at the two dates. This modeling can be used not only to improve the tree-top detection but also to detect changes at tree level (tree cuts and forest regrowth). The experimental results showed that the use of the proposed compound approach improves the tree-top detection compared to what we obtain using only the single date information. This is clearly visible on the lower density data since in that case the exploitation of the richer information content of the higher density data through the compound model is effectively used to recover a significant number of trees. The results showed that the gain in terms of OA achieved on the low density data compared to the single date detection is of 8.6% (i.e., from an OA of 72.6% to an OA of 81.2 %). The analysis also pointed out that simple merging of the two sets of tree-tops is not sufficient to achieve satisfactory results since the merging is not able to detect the changes. This leads to a significant increase of the CE. In contrast, the proposed method solves this problem by automatically handling the detection of forest changes at single tree level. As future work, we plan to test the method on different multitemporal LiDAR datasets and to investigate new geometric features which can further increase the accuracy of the approach.

VI. Acknowledgment

The authors would like to thank the "Dipartimento Risorse Forestali e Montane" of the Autonomous Province of Trento for providing LiDAR data used in this letter in the framework of the FORLIDAR project.

References

[1] C.-S. Lo and C. Lin, "Growth-competition-based stem diameter and volume modeling for tree-level forest inventory using airborne lidar data," *IEEE Transactions on Geoscience and Remote Sensing*, vol. 51, no. 4, pp. 2216–2226, 2013.

[2] J. Stoker, D. Harding, and J. Parrish, "The need for a national lidar dataset," *Photogrammetric Engineering & Remote Sensing*, p. 1067, 2008.

[3] K. Zhao, J. C. Suarez, M. Garcia, T. Hu, C. Wang, and A. Londo, "Utility of multitemporal lidar for forest and carbon monitoring: Tree growth, biomass dynamics, and carbon flux," *Remote Sensing of Environment*, vol. 204, pp. 883 – 897, 2018.

[4] L. Cao, N. C. Coops, J. L. Innes, S. R. Sheppard, L. Fu, H. Ruan, and G. She, "Estimation of forest biomass dynamics in subtropical forests using multi-temporal airborne lidar data," *Remote Sensing of Environment*, vol. 178, pp. 158 – 171, 2016.

[5] Y. Song, J. Imanishi, T. Sasaki, K. Ioki, and Y. Morimoto, "Estimation of broad-leaved canopy growth in the urban forested area using multi-temporal airborne lidar datasets," *Urban forestry & urban greening*, vol. 16, pp. 142–149, 2016.

[6] X. Yu, J. Hyyppä, A. Kukko, M. Maltamo, and H. Kaartinen, "Change detection techniques for canopy height growth measurements using airborne laser scanner data," *Photogrammetric Engineering & Remote Sensing*, vol. 72, no. 12, pp. 1339–1348, 2006.

[7] M. S. Frew, D. L. Evans, H. A. Londo, W. H. Cooke, and D. Irby, "Measuring douglas-fir crown growth with multitemporal lidar," *Forest Science*, vol. 62, no. 2, pp. 200–212, 2015.

[8] D. Marinelli, C. Paris, and L. Bruzzone, "A novel approach to 3-d change detection in multitemporal lidar data acquired in forest areas," *IEEE Transactions on Geoscience and Remote Sensing*, vol. 56, no. 6, pp. 3030–3046, 2018.

[9] C. Paris and L. Bruzzone, "A three-dimensional model-based approach to the estimation of the tree top height by fusing low-density lidar data and very high resolution optical images," *IEEE Transactions on Geoscience and Remote Sensing*, vol. 53, no. 1, pp. 467–480, 2015.

[10] A. Kato, L. M. Moskal, P. Schiess, M. E. Swanson, D. Calhoun, and W. Stuetzle, "Capturing tree crown formation through implicit surface reconstruction using airborne lidar data," *Remote Sensing of Environment*, vol. 113, no. 6, pp. 1148–1162, 2009.